PCCP

RSC Publishing

PAPER

View Article Online
View Journal | View Issue

Cite this: *Phys. Chem. Chem. Phys.*, 2013, **15**, 15981

Energy transfer in coumarin-sensitised lanthanide luminescence: investigation of the nature of the sensitiser and its distance to the lanthanide ion†

Julien Andres and Anne-Sophie Chauvin*

Received 30th May 2013,
Accepted 25th July 2013

DOI: 10.1039/c3cp52279b

www.rsc.org/pccp

A series of lanthanide complexes $[Ln(dpxCy)_3]^{3-}$ have been synthesised. The ligands are composed of a coordinating dipicolinic acid backbone decorated with a polyoxyethylene arm fitted with a coumarin moiety at its extremity. The nature of the coumarin as well as the length of the linker have been varied. Upon excitation at 320 nm, the coumarin exclusively acts as an antenna while the dipicolinic acid core is not excited. Upon excitation below 300 nm, both parts are excited. With europium as a metal centre, the relaxation of the europium ion (intrinsic quantum yield Φ_{Eu}^{Eu} and radiative lifetime τ_r) is constant for all the studied ligands. Therefore, the observed differences in overall quantum yield (Φ_L^{Eu}) in such systems come exclusively from the variation of the terminal coumarin. The overall quantum yields of the studied complexes are low ($\Phi_L^{Eu} < 2\%$ in aqueous solution). In order to rationalise the mechanism of the energy transfer and to improve the sensitisation efficiency (η_{sens}), the distance between the coumarin sensitiser and the lanthanide centre was explored in solution and compared to the solid state. In the solid state, a dramatic effect was confirmed, with an improvement of 80% in the quantum yield Φ_L^{Eu} for short linkers ($(-CH_2CH_2O-)_n$ with $n = 1$ compared to $n = 3$). By monitoring the lifetime decay of the excited state of the lanthanide cation with nanosecond *vs.* microsecond time-resolved spectroscopy at low temperature, the sensitisation of the lanthanide ions by coumarin derivatives was demonstrated to mainly occur through the singlet excited state of the coumarin and not *via* the usual triplet pathway. No evidence of a different behaviour at room temperature was found by transient triplet–triplet absorption spectroscopy.

Introduction

The luminescence of the lanthanide ions is unique and widespread in the different domains that utilise luminescent materials.[1–3] Their photoluminescence however takes place through sensitisation of the lanthanide ion, because the lanthanide ions have very weak extinction coefficients due to the forbidden character of their sharp 4f–4f transitions. The sensitiser absorbs the excitation light and transfers the energy to the lanthanide ions which become excited. Upon relaxation, the lanthanide emits light through luminescence phenomena.[4] Organic chromophores with high extinction coefficients are therefore interesting molecules to ensure an extended harvesting of the excitation light source and can be designed to be incorporated in ligands which strongly coordinate lanthanide ions.

Three strategies ensure a good luminescence of the lanthanide complex, based on different ligand designs.

The first strategy is to design ligands devoid of a chromophoric unit, which strongly coordinate to the lanthanide ion in a 1 : 1 L : Ln ratio (1 ligand per lanthanide ion), and derivatise one of the coordination sites to introduce a sensitiser. Such systems are often based on the 1,4,7,10-tetraazacyclododecane-1,4,7,10-tetraacetic acid backbone (dota) and its cyclen macrocycle, or diethylenetriaminepentaacetic acid (dtpa) and its podant architecture. In those examples, one of the carboxylic acids is typically coupled to a sensitiser by forming an amide bond with this chromophore.[5]

In the second strategy, several chromophoric units are introduced to enhance the extinction coefficient and the architecture allows the presence of several emissive lanthanide centres per complex. This is the case for the dendrimeric polyaminoamine PAMAM.[6]

The third strategy is to directly coordinate the sensitiser to the lanthanide ion. A chromophore with suitable coordination

École Polytechnique Fédérale de Lausanne, ISIC, BCH 1405, CH-1015 Lausanne, Switzerland. E-mail: anne-sophie.chauvin@epfl.ch

† Electronic supplementary information (ESI) available: Luminescence variation of the europium emission upon titration of the dp3Cy ligands with europium, absorption spectra of the free dp3Cy ligands and of their europium complexes, photophysical properties of the $[Tb(dp3Cy)_3]^{3-}$ complexes and of the free dp3Cy ligands including quantum yields Φ_L^{Ln}, Φ_L^L and lifetimes τ_{obs}, fluoresence and phosphorescence spectra of the dpxC1 complexes, derivation of the sensitisation efficiency from the rate of lanthanide population. See DOI: 10.1039/c3cp52279b

sites is therefore needed. Examples include β-diketones and pyridine containing ligands such as dipicolinates among others. This strategy is often adopted because it ensures that the sensitiser is close to the lanthanide ion, which maximises its energy transfer rate.[2]

The energy transfer from the sensitiser to the lanthanide ion is assumed to occur through Dexter's or Förster's mechanism. The rate of the energy transfer depends, in both cases, on the overlap between the donor (sensitiser) and the acceptor (lanthanide ion) energy levels, and on the distance between the donor and the acceptor.[7,8] Dexter's mechanism relies on short range electron exchanges (exponential decay of the energy transfer rate with the separation distance r), whereas Förster's mechanism occurs through longer ranged dipole–dipole couplings (decay proportional to r^{-6}). The actual sensitisation probably occurs in most cases through a complex combination of both mechanisms together with higher order couplings. Excitation energy transfer is indeed still discussed and refined nowadays.[9,10] The particular case of lanthanide sensitisation, where the excitation of the acceptor lanthanide ion is forbidden, was also questioned.[11–13] The dependence of the energy transfer rate on the separation distance between the donor (sensitiser) and the acceptor (lanthanide ion) is nonetheless always present, whatever the mechanism. In this regard, very few examples of a correlation between the distance of the sensitiser relative to the lanthanide ion and the quantum yield of the sensitised emission were highlighted.[14]

The energy transfer in sensitised luminescence of the lanthanide ions is widely accepted to take place mainly from the triplet state of the sensitiser to one of the spectroscopic levels of the lanthanide ion. A certain correlation between the energy of the triplet state of the sensitiser and the quantum yield of the sensitised lanthanide emission was established from various ligands.[15,16] The triplet pathway seems however not mandatory. It has been proven that when the intersystem crossing rate is smaller than about 10^{11} s^{-1}, a singlet transfer mechanism is consistent with the experimental data.[13] Recurrent examples of both near infrared (NIR) and visible light emitting lanthanide ions sensitised through singlet pathways are evidenced in several investigations.[17–19] Furthermore, it was demonstrated that a singlet mechanism is actually interesting to increase the absorption range towards the visible spectrum (the singlet state being higher than the corresponding triplet state, and the Stokes shift between the absorption and the fluorescence being smaller than between the absorption and the phosphorescence).[19] Besides the sensitisation pathway(s) and the associated mechanism(s) of energy transfer, there are many deactivation (or relaxation) pathways that are in competition with the sensitisation of the lanthanide ion. For all these reasons, the relationship between the photophysical properties of the sensitiser and those of the corresponding luminescent lanthanide complex is fairly intricate and any conclusion should always be made with caution.

We propose here a versatile strategy that enables investigating different fundamentals of the sensitisation of the lanthanide ions with simple complexes based on coumarins as sensitisers coupled to a derivative of dipicolinic acid (dpa) as a coordinating moiety. We elucidate the sensitisation pathways in such complexes by spectroscopic techniques and show how the ligands can be tuned to improve the efficiency of the sensitisation and of the luminescence of the lanthanide ion.

Design and synthesis of the ligands

The design of the ligands was carried out to allow investigating the influence of several sensitisers without disrupting the coordination sphere. One of the major problems when comparing different sensitisers is that the coordination sphere and therefore the ligand field around the lanthanide ion often depend on the sensitiser. It has been indeed proven that the radiative lifetime of the lanthanide excited states mainly depends on the refractive index of the medium and on the coordination environment of the lanthanide ion.[20] It is hence difficult to conclude whether an improved emission of the luminescent lanthanide ion is due to the coordination, to the structure of the ligand, to its photophysical properties or to a combination of these contributions.

In order to minimise the effect of the coordination sphere, we chose to exclude the sensitiser from the first coordination sphere. We opted for a coordination site formed by the dipicolinate (dpa) framework, which forms 3 : 1 L : Ln complexes under stoichiometric conditions. The chromophore of the dpa framework is a classic example of a good sensitiser of several lanthanide ions. Nevertheless, its absorption is limited to short-wave UV light below 300 nm. A distant sensitiser that would absorb higher than 300 nm would thus be exclusively excited (*i.e.* no excitation of the dpa moiety at λ_{ex} > 300 nm). We chose here coumarins as sensitisers absorbing above 300 nm, yet below 400 nm to ensure that the excited state is not too low (which would preclude any sensitisation). The sensitiser was grafted at the *para* position of the dipicolinate moiety, with a linker in between the dpa moiety and the sensitiser. The tridentate dipicolinate coordination site was preferred to a dota or dtpa one because of its well defined tris structure forming a nine-coordinated lanthanide complex (whereas dota and dtpa are seven or eight-coordinated and include, in aqueous solution, one or two water molecules in the first coordination sphere), because of its ability to sensitise the lanthanide ion by excitation below 300 nm (yet not exploited here), and because of the good stability of its lanthanide complexes and rapid complexation in aqueous solution (see the Experimental section).[21]

There are a few examples of coumarin-sensitised lanthanide luminescence in the literature. Most of these examples involve macrocyclic crown ethers, or the direct coordination of a coumarin.[22–27] Féau *et al.* were particularly prolific with coumarin-sensitised lanthanide complexes, showing nice examples of coumarins as sensitisers in polyaminocarboxylate complexes.[28,29] An analyte responsive luminescent probe based on an analyte-triggered formation of a coumarin sensitiser was also published recently by Borbas and co-workers.[30] Finally, ligands with quinolinone sensitisers were studied by Sevlin and co-workers.[31–34] The structure of quinolinones is close to the one of coumarins, the endocyclic oxygen atom of coumarins being replaced by an amine in quinolinones.

We chose polyoxyethyene arms (POE, x = 1–3) as linkers between the sensitiser and the coordination site. This choice was motivated by its water-soluble compatibility, by the absence of conjugation with the dpa moiety or other chromophoric bridges, and by the characterisation of lanthanide complexes based on similar structures (without the sensitiser at the end of the side chain).[35] This approach is therefore different from other designs involving dpa derivatives, for example as undertaken by Maury *et al.*, who have developed highly conjugated systems with a donor–acceptor effect for two photon microscopy.[36]

The general structures of the ligands and corresponding complexes are depicted in Scheme 1. In solid states, the POE side chains usually adopt a *trans–gauche–trans* conformation at each $-CH_2CH_2O-$ unit, which forms helical structures.[37] In solution, the movement (diffusion) of polymer pendent arms grafted on a surface generally describes mushroom structures at room temperature when the density of the polymer pendent arms is low (brush structure at high density).[38] The position of the sensitiser at the end of the side chain relative to the lanthanide ion is hence certainly quite flexible; nevertheless, the sensitiser is clearly not in direct contact with the lanthanide ion because of the three dpa moieties that already fill the coordination sphere. Furthermore, in their investigation of trioxyethylenated dpa derivatives, Gassner *et al.* did not observe any folding of the POE side chain in the dp3OMe ligand and in the $[Lu(dp3OMe)_3]^{3-}$ complex in solution by ROESY-NMR spectroscopy.[35]

We recently published a first investigation of one such complex with a 4-methylumbelliferone (4-methyl-7-hydroxycoumarin) fluorophore at the end of a trioxyethylene side chain (x = 3).[39] This investigation focused on the different sensitisation pathways depending on the excitation wavelength and confirmed that this ligand architecture does not preclude the sensitisation of the lanthanide ion. However, the sensitisation efficiency was found to be lower when exciting the distant coumarin (at 320 nm) compared to the simultaneous excitation of the dpa and coumarin moieties (at 270 nm). Furthermore, the efficiency of the europium sensitisation was rather low and was attributed (i) to a poorly located triplet state energy of the donor relative to the europium acceptor spectroscopic levels, and (ii) to the length of the side chain that can extend up to ~15 Å. The double sensitisation ability was yet an interesting way to modulate the ratio between the coumarin blue fluorescence and the red luminescence of the europium ion by changing the excitation wavelength.

In the present article, we only focus on an excitation at 320 nm. This excitation exclusively populates the distant sensitiser (the coumarin). Therefore, the dpa moiety is essentially acting only as a coordination site. However, this does not mean that the dpa moiety is not involved in the sensitisation process. Its contribution is yet believed to be identical in all our complexes, because of its stable and well defined coordination site that should be unaffected by the distant coumarin, as reported previously.[39]

To further test the assumptions regarding the poor sensitisation efficiency of the already reported distant coumarin, we decided

(i) to change the nature of the sensitiser for different coumarins and (ii) in parallel, to shorten the $-(CH_2CH_2O)_x-$ linker.

The different ligands are presented in Scheme 1. They will be referred to as ''dpxCy'' hereafter where ''px'' refers to the length of the side chain (x = 1–3), and ''Cy'' to the nature of the sensitiser (coumarins, y = 1–5).

The synthesis of the ligands is performed in four steps. The first step consists in the coupling of the sensitiser with the POE side chain. A nucleophilic functional group – an acidic hydroxyl at the seventh or fourth position on the coumarin core – reacts with a tosylated oligoethylene glycol monomethyl ether. The terminal monomethyl ether is then cleaved by trimethylsilyl iodide (TMSI), thus forming the terminal alcohol. This alcohol is grafted on a chelidamic diester through a Mitsunobu coupling. Because the coupled diester is hard to purify by chromatography without a massive loss of compounds, the Mitsunobu coupling has to be as clean as possible, in order to ensure that it can be used directly in the next step. We found that using polymer-supported triphenylphosphine (PS-TPP) instead of free triphenylphosphine is a very convenient way to guarantee a minimal amount

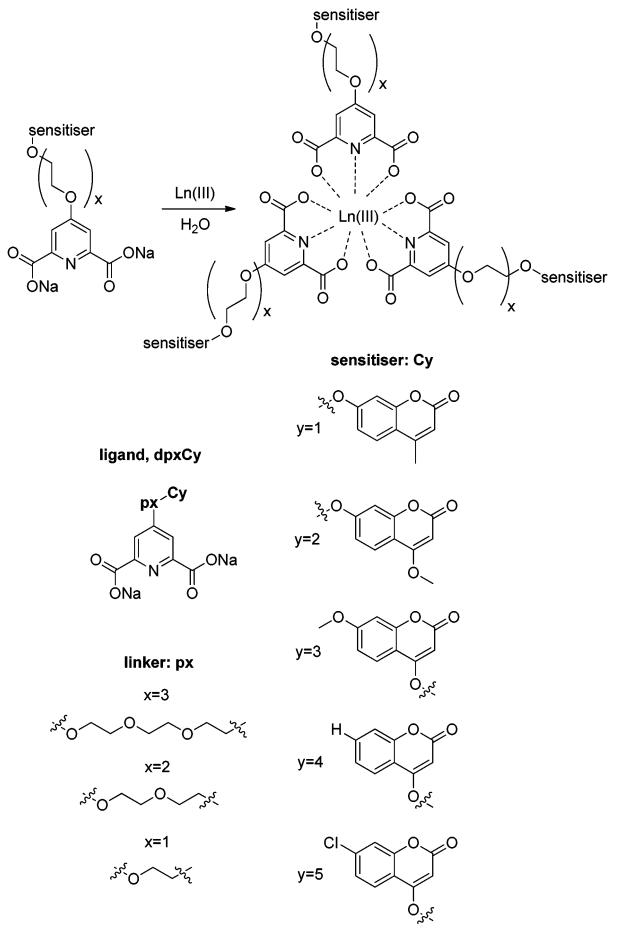

Scheme 1 Ligand design forming tris complexes with lanthanide ions in water (pH 7.4) and allowing the variation of the sensitiser and of the length (x = 1–3) of the polyoxyethylene (POE) side chain. Structures of the dpxCy ligands. Studied variation of the nature of the sensitiser Cy (coumarins) and of the length of the px linker (POE side chain).

of impurities in the ligand diester precursor, since the polymer can be easily filtered out of the solution. To be certain that no residual uncoupled chelidamic diester is present in the crude product of the Mitsunobu reaction, an excess of coumarin–oligoethylene glycol is used, and the complete disappearance of the uncoupled chemidamic diester is checked by TLC and by ^{1}H-NMR spectroscopy. The final step is the deprotection of the carboxylic esters to form the carboxylates. The hydrolysis is carried out in ethanol upon addition of an aqueous solution of sodium hydroxide. The sodium salt of the ligand, which precipitates in ethanol, can then be further purified by a series of precipitations in ethanol. This procedure ensures the complete removal of impurities resulting from the Mitsunobu reaction (mainly of the excess of coumarin–oligoethylene glycol) as proven by NMR spectroscopy and microanalysis: the impurities being soluble in ethanol, while the carboxylate ligand is not. Five different coumarins were coupled to dpa in this way, using triethylene glycol as a side chain. One coumarin (4-methylumbelliferone) was coupled to the dpa moiety using three different POE linkers (triethylene, diethylene and ethylene glycol) according to the same synthetic strategy. Each ligand was characterised by NMR spectroscopy, Electrospray Ionisation Mass Spectrometry (ESI-MS) and microanalysis. The lanthanide complexes were directly prepared in aqueous solution by adding the stoichiometric amount of lanthanide ions (from a titrated solution of a lanthanide salt) to a Tris-buffered solution at pH 7.4 of the diluted ligand. This is the normal procedure reported in the literature for the preparation of 3 : 1 L : Ln lanthanide complexes with dpa derivatives.[21]

The investigation of the photophysical properties of the ligand-centred and metal-centred emission was carried out in Tris-buffered aqueous solutions at pH 7.4 (concentration of 0.1 mM in lanthanide complexes). Such a pH value and concentration range were demonstrated to be well suited for the luminescence of the dp3C1 complexes[39] and sustain the high stability of the [LnL_3] species with similar complexes (the stability is comparable whatever the lanthanide ion).[21,35]

Variation of the sensitiser: coumarin derivatives

Formation of the complexes in aqueous solution

Dp3C1 and a series of polyoxyethylenated dpa ligands were already reported elsewhere to form stable 3 : 1 L : Ln complexes.[30,39] Their formation was investigated by NMR spectroscopy, ESI-MS, UV-Vis spectrophotometry and luminescence. In this study, we do not report once more the full characterisation of the complexes, but we illustrate their stability by luminescence comparatively to already reported results.

The formation of the complexes in solution was verified by monitoring the emission of the lanthanide ion upon titration of the dp3Cy ligands with Eu(III) (see Fig. S1, ESI†). A maximum of the emission is reached at a ligand to lanthanide ratio (L : Ln) of 3 : 1, thus indicating that the [LnL_3] species (tris species) should form predominantly under stoichiometric conditions. The tris species is the most luminescent species in solution because of the absence of quenching water molecules in the coordination sphere of the lanthanide ion.[21,40] The lifetimes from the emissions at a L : Eu ratio of 3 : 1 are all around 1.4 ms ± 0.1 ms. Such lifetimes are typical for the relaxation of europium through f–f transitions in dpa complexes without water molecules in the first coordination sphere. The parent dpa ligand exhibits for example a lifetime of 1.6 ms for its tris species and 0.3 ms for its tris-hydrated bis species.[21,40] With the dp3Cy containing complexes, the lifetimes at 1.4 ms are well fitted by monoexponential decays; the [LnL_3] species are then the major luminescent species in solution under those conditions. This result is in agreement with data obtained on similar structures by different techniques such as NMR spectroscopy, UV-vis absorbance spectroscopy and time-resolved spectroscopy.[21,35] The dpa coordination site is then, as expected, not sterically hindered by the distant coumarins. The variation of the terminal coumarin has no impact on the formation of the lanthanide complexes.

Absorption of the different coumarins

The absorption of the europium complexes are presented in Fig. 1 together with the absorption of each coumarin (for comparison purposes, grafted to the POE side chain but without the dpa moiety). The presence of the coumarins extends the absorption range from below 300 nm (absorption of the dpa moiety) up to 360 nm. The shapes of the coumarin absorptions above 300 nm are practically unaffected by the coupling to the dpa coordination site and by the complexation of the ligands to the europium ion (Fig. 1 and Fig. S2–S6 of the ESI†). Even though the extinction coefficients of the maxima (attributed to

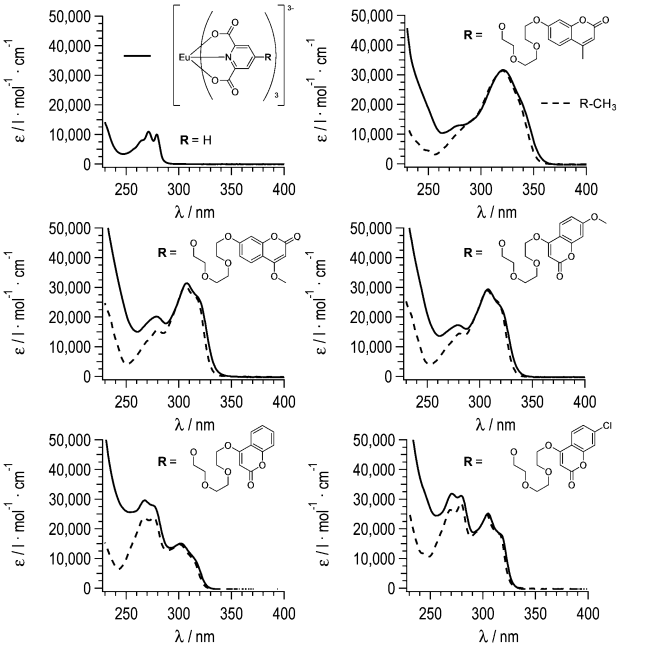

Fig. 1 Molar extinction coefficients of the $[Eu(dp3Cy)_3]^{3-}$ complexes (plain) and the corresponding coumarin-trioxyethylene monomethyl ether (dashed) scaled to show their absorption range in the complexes. Aqueous Tris-buffered solution (0.1 mM in complex), pH 7.4.

$\pi \rightarrow \pi^*$ transitions) are changed upon coordination (values reported in Table S1 of the ESI† for the europium complexes), when the absorption spectra are scaled at the maximum of the coumarin absorption, only small differences between the peak and shoulder of the absorption of the coumarin moieties above 300 nm are observed. This behaviour was anticipated because the coumarins are not directly involved in the coordination, which is performed by the dpa moiety. On the parent dpa, the coordination indeed induces an increase of the extinction coefficient, a narrowing of the transitions, and a small bathochromic shift (red-shift) as shown in Fig. S2 of the ESI.† However, those effects are not observed with the dp3Cy ligands in the absorption range of the dpa chromophore because the superposed absorptions of the coumarins mask the absorption structure of the dpa moiety.

Besides those coordination consequences, an essential result is that an excitation above 300 nm (*e.g.* 320 nm) only populates the coumarins, because the dpa moiety absorbs only below 300 nm. In order to solely investigate the sensitisation through the coumarins, all photophysical measurements are performed under excitation at 320 nm. From a comparative study of the direct excitation of the coumarin *versus* the double excitation of the dpa and coumarin moieties, the results are found to be similar to those already reported with the dp3C1 ligand.[39]

Ligand-centred photophysical properties

The ligand-centred emissions from the gadolinium complexes (non emissive under those conditions) upon variation of the terminal coumarin are shown in Fig. 2. The fluorescence from the singlet state (S_1) was measured at room temperature, whereas the phosphorescence from the triplet state (T_1) was recorded at 77 K, 50 μs after a pulsed irradiation.

According to the data in Table 1, a correlation exists between the structure of the coumarin and the location of its excited states. For instance, dp3C2 and dp3C3 only differ by the coupling position on the coumarin, seventh *vs.* fourth respectively, and are characterised by the same singlet and triplet values (singlet at 27 000 cm^{-1} and triplet at 23 500 cm^{-1}). However, a similar value for the singlet state of two ligands does not imply that the triplet states are located at the same energy. For example, dp3C4 and dp3C5 have a first excited singlet state at the same position (*i.e.* 28 000 cm^{-1}), but a first triplet excited state that is slightly shifted by calc. 500 cm^{-1}. It probably comes from a slightly better stabilisation of the triplet excited state in the dp3C5 structure (7-chloro) compared to the dp3C4 structure (unsubstituted seventh position).

Table 1 Location of the singlet (S_1) and triplet (T_1) excited state of the dp3Cy ligands in their gadolinium complex in wavenumber (±300 cm^{-1})

$[Gd(dp3Cy)_3]^{3-}$	S_1(max)/cm^{-1}	T_1(0–0)/cm^{-1}
$y = 1$	26 000	21 500
$y = 2$	27 000	23 500
$y = 3$	27 000	23 500
$y = 4$	28 000	23 500
$y = 5$	28 000	23 000

Metal-centred photophysical properties

The metal-centred emissions from the europium complexes upon variation of the terminal coumarin are shown in Fig. 3. They all exhibit the characteristic europium $^5D_0 \rightarrow {}^7F_J$ f–f transitions (J = 1–4) under excitation at 320 nm, meaning that the europium is sensitised by each coumarin (so-called antenna effect). A residual fluorescence of the coumarin is also observed alongside. These short-lived coumarin emissions are absent on time-resolved spectra when a delay of a few microseconds is applied between the pulsed excitation and the measurement.

The efficiencies of the ligand-centred and metal-centred emissions for the europium complexes are presented in Table 2 (for terbium, see Table S2 of the ESI†). The europium complexes are particularly useful because additional photophysical properties, which are not easy to find for the other lanthanide ions, can be extracted from the intensity of the $^5D_0 \rightarrow {}^7F_1$ transition

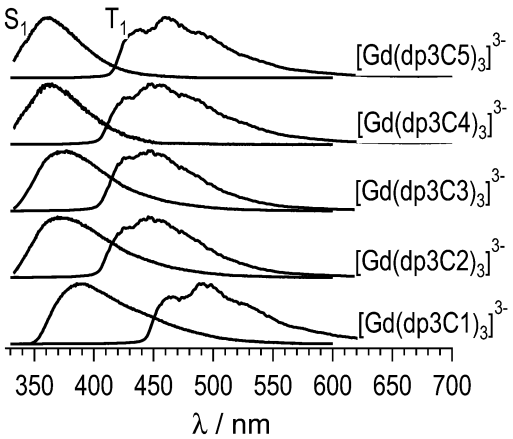

Fig. 2 Fluorescence from S_1 and phosphorescence from T_1 of the $[Gd(dp3Cy)_3]^{3-}$ complexes (λ_{ex} = 320 nm). Aqueous Tris-buffered solution (0.1 mM in complex), pH 7.4 (S_1), and frozen solution at 77 K (10% glycerol added), 50 μs after a pulsed irradiation (T_1).

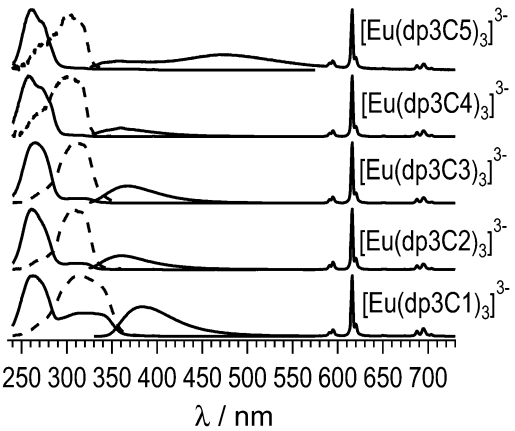

Fig. 3 Excitation (left hand side, plain for the Eu-centred emission, dashed for the residual coumarin emission) and emission spectra (right hand side, λ_{ex} = 320 nm) of the $[Eu(dp3Cy)_3]^{3-}$ complexes (0.1 mM) in Tris-buffered aqueous solution, pH 7.4.

Table 2 Photophysical properties of the $[Eu(dp3Cy)_3]^{3-}$ and $[Gd(dp3Cy)_3]^{3-}$ complexes at room temperature (λ_{ex} = 320 nm). τ_{obs}^{Eu} = 1.4 ms ± 0.1 ms, τ_r^{Eu} = 4.2 ms ± 0.4 ms Φ_{Eu}^{Eu} = 33% ± 5%, for all complexes in this table. Estimated error of 10% on the quantum yields (sensitised quantum yields of the europium emission Φ_L^{Eu}, quantum yields of the ligand-centred emission Φ_L^L)

	Ln = Eu		Ln = Gd	
$[Ln(dp3Cy)_3]^{3-}$	Φ_L^{Eu}/%	Φ_L^L/%	η_{sens}/%	Φ_L^L/%
y = 1	1.7	7.7	5.1	9.1
y = 2	0.4	0.9	1.2	1.1
y = 3	0.7	1.1	2.1	1.6
y = 4	n.d.	n.d.	<0.6	n.d.
y = 5	0.3	n.d.	0.8	n.d.

N.d. values were too low to be determined with the experimental setup.

relative to the total intensity from the $^5D_0$ spectroscopic level. The $^5D_0 \rightarrow {}^7F_1$ transition has indeed a purely magnetic dipole (MD) nature and no electric dipole (ED) character. This unique characteristic simplifies the determination of the radiative lifetime of europium, see eqn (1).[41] This equation assumes that the strength and energy of the MD transition is constant and independent on the environment around the europium ion and therefore, that the radiative rate depends only on the ratio of the MD transition relative to the total emission from the $^5D_0$ spectroscopic level, and on the refractive index of the medium.

$$\frac{1}{\tau_r} = k_r = A_{MD,0} \cdot n^3 \cdot \frac{I_{tot}}{I_{MD}} \quad (1)$$

From the radiative lifetimes, other parameters such as the intrinsic quantum yield (Φ_{Ln}^{Ln}), which corresponds to the quantum yield by direct excitation of the lanthanide ion (without the losses from the sensitisation pathways), and the sensitisation efficiency (η_{sens}) can be calculated according to eqn (2) and (3).

$$\Phi_{Ln}^{Ln} = \frac{\tau_{obs}}{\tau_r} \quad (2)$$

$$\Phi_L^{Ln} = \eta_{sens} \cdot \Phi_{Ln}^{Ln} \quad (3)$$

We observe from the emission spectra on Fig. 3, that all the europium emission spectra have exactly the same shape. Consequently, the radiative lifetimes τ_r calculated from eqn (1) are all identical (4.2 ms) whatever the terminal coumarin. This result is consistent with other results found in the literature (from europium complexes of dpa derivatives as well as of other types of ligands), which seems to indicate that the radiative lifetime depends mostly on the coordination sphere and on the neighboring environment.[20,35] The observed lifetime τ_{obs} (defined as the inverse of the sum of the radiative rate constant with all other deactivation rate constants), which is fitted from the exponential decay of the emission after a pulsed excitation, is also indistinguishable at 1.4 ms (within experimental error) for all the complexes in Table 2. These lifetimes are similar to those of other dpa derivatives. As a consequence, the intrinsic quantum yield, which represents the efficiency of the radiative deactivation of the lanthanide ion relative to all its deactivations, has to be the same for each $[Eu(dp3Cy)_3]^{3-}$ complex. This suggests that the deactivation of the europium ion does not involve the distant sensitiser. Therefore, we can fairly assume that the difference in quantum yields Φ_L^{Eu} between the complexes in Table 2 is only due to the difference in sensitisation efficiency.

This conclusion is however limited to these $[Eu(dp3Cy)_3]^{3-}$ complexes. A comparable study was performed with the terbium complexes (see Table S3, ESI†), and points to a strong deactivation of the terbium excited state for one of the terminal coumarin. This was demonstrated with the short observed lifetime for the $[Tb(dp3C1)_3]^{3-}$ complex (0.6 ms ± 0.1 ms). This is expected because the dp3C1 ligand has the lowest excited states (either singlet at 26 000 cm^{-1} or triplet at 21 500 cm^{-1}). The $^5D_4$ spectroscopic level of terbium(III) being located at 20 500 cm^{-1}, a back-transfer seems highly probable. This also explains why both the dp3C2 and dp3C3 ligands, with higher excited states, are better than dp3C1 for the terbium sensitisation (Φ_L^{Tb} = 1.4% and 1.7% *versus* 0.5% respectively).

Eventually, for europium(III) the $^5D_2$ spectroscopic level, located at 21 500 cm^{-1}, is at the same energy as the triplet of dp3C1. Since no particular deactivation relative to the other complexes was observed here, it strongly suggest that the energy transfer occurs on a lower spectroscopic level such as the $^5D_1$ (at 19 000 cm^{-1}) or the emissive $^5D_0$ (calc. 17 223 cm^{-1} from the high resolution measurement of the $^5D_0 \leftarrow {}^7F_0$ transition of $Cs_3[Eu(dp3C1)_3]$).[39]

A comparison of the ligand-centred quantum yields of the non-emissive gadolinium complexes Φ_L^L(Ln = Gd) with those of the emissive europium complexes Φ_L^L(Ln = Eu), reveals that the ligand-centred quantum yields of the gadolinium complexes are always higher than those of the corresponding europium complexes. A certain correlation exists between the ligand-centred quantum yield of the non-emissive complex Φ_L^L(Ln = Gd) with the corresponding europium-centred sensitised quantum yield Φ_L^{Eu}. When the ligand-centred quantum yield was too low to be measured, the europium quantum yield was also at the threshold limit of our setup. The emission from the dp3C1 ligand in the gadolinium complex (9.1%) results in the highest europium quantum yield of the series (1.7%). The lower emission from the dp3C2 and dp3C3 ligands (1.1–1.6%) yields lower quantum yields (0.4–0.7%), whereas the very few emitting dp3C4 and dp3C5 ligands have a very weak europium emission. An expected quenching of the ligand emission by the emissive lanthanide ion is however observed when measurable.

These first results obtained by variation of the distant sensitiser indicate several important limitations of the sensitisation process. First of all, an appropriate energy difference between the acceptor spectroscopic level of the lanthanide ion and the donor excited states of the sensitiser is a very important limitation and has to be optimised to maximise the sensitisation efficiency. This was demonstrated by pointing out the strong deactivation of the terbium excited state in the ligand with the lowest excited states. When this limitation is overcome, the sensitisation is then limited by the structure of the sensitiser. Small changes on a same backbone can indeed have drastic impacts on the photophysics of this molecule. For example, it is well known that the incorporation of a heavy

atom such as a bromine or an iodine atom on a fluorophore increases the intersystem crossing rate by spin–orbit coupling.[42] In our case, we observed that several complexes with similar excited states but different structures exhibit completely different quantum yields. The limitation is then probably the competing deactivation processes, and particularly the quenching of each sensitiser by its environment.

The sensitisation efficiency, which is defined as the ratio of the number of sensitised lanthanide ions per number of excited sensitisers, can be divided into several contributions according to the sensitisation pathways. For a sensitisation through the triplet state of the sensitiser, it is defined as the product of the intersystem crossing efficiency, η_{isc} (number of triplet states populated per number of excited singlet states), by the energy transfer efficiency, η_{et} (number of sensitised lanthanide ions per number of triplet state sensitisers). To better understand the sensitisation process, the rate constants of each photophysical phenomenon must be considered, because the sensitisation is in competition with many different deactivation pathways. To maximise the sensitisation efficiency, the energy transfer rate constant has to be as high as possible compared to the other deactivations, ideally much higher, so that the other processes can be neglected, which would yield a sensitisation efficiency of 100%.

The rate constant of the energy transfer is assumed to depend on the overlap between the donor state of the sensitiser and the acceptor state of the lanthanide ion, as well as on the distance between the donor and the acceptor. We have already illustrated the importance of the energy of the excited states in this first part, but we also pointed out the importance of the competing processes that can easily overcome the energy transfer rate. In an attempt to rationalise the mechanism of the energy transfer in a sensitised luminescent lanthanide complex, we undertook a shortening of the POE side chain in our original ligand that exhibits the best photophysical properties in the series of Table 2, *i.e.* dp3C1. We then synthesised ligands dp2C1 and dp1C1 (Scheme 1) and investigated the photophysical properties of their respective europium complexes.

Variation of the length of the linker

Photophysical properties in aqueous solution and in the solid state

In aqueous solution, all the $[Eu(dpxC1)_3]^{3-}$ (x = 1–3) complexes exhibit the same characteristic red emission from the europium centre as well as the residual coumarin emission. The ligand-centred fluorescence and phosphorescence spectra are unchanged upon variation of the length of the side chain (same as Fig. 2, with $[Gd(dp3C1)_3]^{3-}$ at 26 000 and 21 500 cm^{-1}, see Fig. S7 of the ESI†), meaning that any difference in metal-centred photophysical properties ought to be due to the shorter side chain and not to a different location of the donor excited state. The quantum yields together with other photophysical properties of the corresponding $[Ln(dpxC1)_3]^{3-}$ (x = 1–3) complexes are presented in Table 3.

Unexpectedly, the shortening of the side chain has practically no influence on the quantum yield Φ_L^{Eu} in aqueous solution, which remains between 1.2% and 1.8% (see Table 3). The ligand with the intermediate length (dp2C1) seems even slightly less efficient than the other two ligands with a quantum yield Φ_L^{Eu} = 1.2%. This suggests that any increase of the energy transfer rate that would be due to the shorter side chain (if any), would be compensated by a decrease of another component of the sensitisation efficiency, or of the europium intrinsic quantum yield. In terms of rate constants, it then corresponds to a competitive process that deactivates the sensitiser or the europium ion.

Table 3 Photophysical properties of the $[Eu(dpxC1)_3]^{3-}$ and $[Gd(dpxC1)_3]^{3-}$ complexes at room temperature in aqueous solution (aq) and in solid state (s). λ_{ex} = 320 nm. τ_{obs}^{Eu} = 1.4 ms ± 0.1 ms, τ_r^{Eu} = 4.2 ms ± 0.4 ms (aq) and 2.8 ms ± 0.4 ms (s), Φ_{Eu}^{Eu} = 33% ± 5% (aq) and 50% ± 5% (s), for all complexes in this table. Estimated error of 10% on the quantum yields (sensitised quantum yields of the europium emission Φ_L^{Eu}, quantum yields of the ligand-centred emission Φ_L^L)

	Ln = Eu						Ln = Gd	
	Φ_L^{Eu}/%		Φ_L^L/%		η_{sens}/%		Φ_L^L/%	
$[Ln(dpxC1)_3]^{3-}$	aq	s	aq	s	aq	s	aq	s
x = 3	1.7	4.5	7.7	5.6	5.1	9.0	9.1	6.1
x = 2	1.2	6.8	6.3	5.7	3.6	13.6	7.1	6.3
x = 1	1.8	25.2	14.7	7.8	5.4	50.4	15.5	10.7

In order to identify why the shortening of the side chain has no real impact on the quantum yield in aqueous solution, the following strategies were adopted. First, quenching phenomena were decreased by studying solid state samples and by freezing the aqueous solutions at 77 K. This strategy suppresses most of the quenching due to the presence of water molecules, and lowers the rate constants of diffusion limited quenching phenomena, respectively. The mechanisms of the sensitisation were then investigated through time-resolved spectroscopy. The chemical environment of the complexes changes quite a lot once in the solid state (compared to the situation in aqueous solution). The refractive index is higher in the solid state (1.517 from ref. 43 *versus* 1.333 in water); there is a high density of complexes probably in close contact, and a more rigid environment than in solution.

The ligand-centred and metal-centred photophysical properties of the solid state samples were measured from the solid state samples and not extrapolated from the aqueous solution. As seen in Table 3, nearly all photophysical properties are altered relative to those in aqueous solution.

The trend in the solid state demonstrates the expected behaviour when the side chain is shortened, *i.e.* an increase of the quantum yield. The quantum yield Φ_L^{Eu} increases up to 25% when the sensitiser is only separated from the coordination site by one $-CH_2CH_2O-$ unit. The shape of each characteristic europium emission in the solid state is very similar throughout the series, so that the radiative lifetime can be estimated to be fairly identical for the three complexes. Since the observed lifetime is also not altered, the intrinsic quantum yield stays at 50%. The difference in sensitised quantum yield then ought to come from an increased sensitisation efficiency, and presumably from a higher energy transfer rate.

Noteworthily, the emission from the coumarin seems also to be affected by the length of the side chain. This is even true in

aqueous solution where the quantum yield of the coumarin emission is twice that of the ligands with the longer linkers. This last point stresses one of the major problems of any system that tries to investigate the relationship between the distance of a donor–acceptor and the rate of the energy transfer: at close distances, the environment of the donor and of the acceptor is altered by the presence of its partner. In our case, the presence of the coordination site seems somehow to increase the efficiency of the coumarin emission, which means either that the radiative lifetime of the coumarin is increased, or that the quenching and/or non-radiative relaxations are decreased. By measuring the lifetimes of the europium $^5D_0$ spectroscopic level at 77 K, we also noticed that it jumped from 2.2 ms with the longer linkers up to 4.7 ms for the shortest side chain, while the room temperature lifetimes in aqueous solution are similar within experimental error (at 1.4 ms ± 0.1 ms). This result strongly suggests that the efficiency in aqueous solution is limited by the quenching from diffusing solvent molecules, and that when the coumarin is close to the coordination site and frozen it may also participate in the second coordination sphere and help prevent the non-radiative deactivations of the europium ion. The lifetime of 4.7 ms is indeed what may be expected from a purely radiative relaxation since the radiative lifetime was calculated in aqueous solution at 4.2 ms (the radiative lifetime is identical with the three ligands).

The fact that the quantum yield Φ_L^{Eu} is unchanged upon shortening of the linker may also be understood as a proof that the sensitiser is standing at a similar average distance from the lanthanide ion in aqueous solution and at room temperature, which should be at the upper limit the length of the shortest side chain (~5 Å). It would mean that the POE side chain may be fairly folded rather than extended. On the other hand, it may also come from a diffusion limited energy transfer. The excited sensitiser at the end of the side chain moves around the complex until the energy transfer rate is sufficiently high, and therefore until the sensitiser is close enough to the lanthanide ion, to allow an excitation transfer onto the lanthanide ion. Those phenomena would be removed in the solid state since the structure is in that case more rigid and hence better defined. The increased quantum yield of the coumarin emission Φ_L^L for the complex with the shortest side chain (*i.e.* with the dp1C1 ligand) in aqueous solution could then be understood as a decreased self-quenching of the coumarin by the other coumarin moieties on the two remaining ligands of the complex. Self-quenching was indeed observed in a previous study to be a significant deactivation process in the $[Eu(dp3C1)_3]^{3-}$ complex.[39] This decreased self-quenching in the dp1C1 complex could be due to a limited diffusion range when the linker is smaller, thus restricting the contact of the coumarin moieties within the complex.

Time-resolved luminescence: a tool for deciphering the sensitisation pathway

There are actually two possible pathways that yield an energy transfer, the singlet S pathway, and the triplet T pathway, which both occur from the corresponding singlet or triplet excited states of the sensitiser. The singlet pathway is most of the time neglected. However, efficient energy transfers were already observed from the singlet excited state.[17–19] Both contributions should hence be considered first. The major one can then be determined by observing whether a quenching of the triplet state is observed in a luminescent lanthanide complex relative to a corresponding non-luminescent lanthanide complex. The sensitisation efficiency should therefore contain the contribution from the singlet state η_{et}^S, as well as the contribution from the triplet state η_{et}^T. The sensitisation efficiency should thus be approximated as in eqn (4) (for the complete derivation from the rate of lanthanide population, see ESI†).

$$\eta_{sens} = \eta_{et}^S + \eta_{et}^T \cdot \eta_{isc} \quad (4)$$

Each of those parameters can be expressed in terms of the rate constant as the ratio of the considered process relative to all the deactivations of the associated excited state as shown in eqn (5).

$$\eta_{isc} = \frac{k_{isc}}{k_{obs}^S}, \quad \eta_{et}^S = \frac{k_{et}^S}{k_{obs}^S}, \quad \eta_{et}^T = \frac{k_{et}^T}{k_{obs}^T} \quad (5)$$

The sum of all the deactivations of the associated excited state k_{obs} can be approximated as in eqn (6), where k_f is the fluorescence radiative lifetime, k_p the phosphorescence radiative lifetime and k_{nr} the sum of all the non-radiative deactivations of the excited state.

$$k_{obs}^S = k_f + k_{isc} + k_{et}^S + k_{nr}^S$$
$$k_{obs}^T = k_p + k_{et}^T + k_{nr}^T \quad (6)$$

The observed relaxation rate constants k_{obs} are usually expressed as their inverse, which gives observed lifetimes τ_{obs} (eqn (7)).

$$\tau_{obs} = \frac{1}{k_{obs}} \quad (7)$$

In order to determine whether a preferential sensitisation pathway is followed in our case, the sensitisation mechanisms were studied by time-resolved spectroscopy both for the solid state samples and for the frozen aqueous solution at 77 K.

On the nanosecond time-resolved emission spectra of the solid state and frozen solution, the fluorescence from the coumarin is observed together with the transitions from the higher $^5D_1$ spectroscopic level of europium. The transitions from the typical $^5D_0$ state are however absent. It then means that the energy transfer most probably occurs mainly on the $^5D_1$ level, which lies ~1700 cm^{-1} higher than the $^5D_0$ level. In the microsecond time scale (see Fig. 4), the $^5D_1$ emission bands decrease while the $^5D_0$ peaks rise.

The decay rates of the $^5D_1$ level are identical (within experimental error) for all the ligands in the dpxC1 series, with a lifetime of 1.3 μs ± 0.2 μs. This decay is also observed on the parent dipicolinate complex, so that it seems to be defined mostly by the coordination sphere. The rise time of the transitions from the $^5D_0$ level is in the same range as the decay time

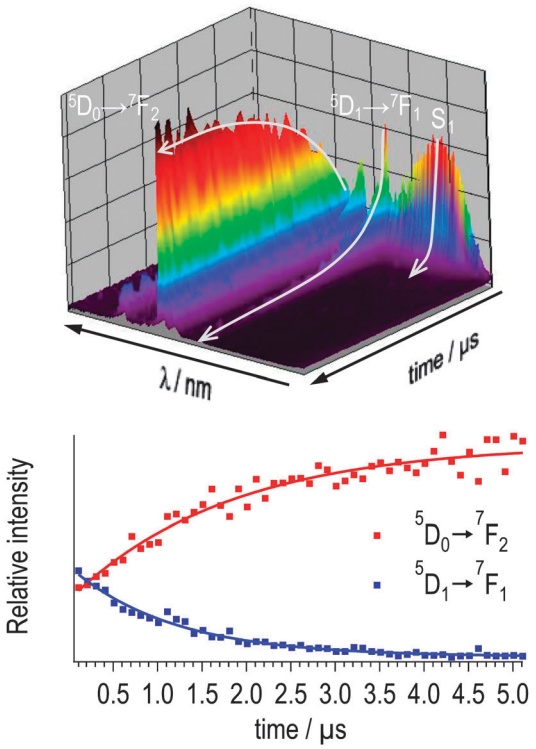

Fig. 4 Time-resolved emission spectrum of $Na_3[Eu(dp3C1)_3]$ in the solid state (λ_{ex} = 320 nm) and the extracted decay of the $^5D_1$ and rise of the $^5D_0$ spectroscopic levels.

of the $^5D_1$ level. It is therefore obvious that the energy is first transferred from the sensitiser onto the $^5D_1$ level and from there onto the $^5D_0$ level.

In aqueous solution and at room temperature, the emission from the $^5D_1$ level is very difficult to observe (very weak intensity). It probably comes from the rapid quenching of this level by water molecules, which relax the europium ion down to the $^5D_0$ spectroscopic level. Water has indeed a vibrational bending transition at 1645 cm^{-1}, which would be a good acceptor for the energy gap between the $^5D_1$ (19 000 cm^{-1}) and the $^5D_0$ states (17 223 cm^{-1}, from ref. 39).

By increasing the time scale up to milliseconds, the decay of the $^5D_0$ spectroscopic level of the europium ion down to the ^7F_J spectroscopic levels is clearly seen by the luminescence decays of the characteristic transitions. This decay is observed at low temperature in frozen solution, in the solid state at room temperature and in aqueous solution at room temperature.

In order to observe the phosphorescence of the ligand, low temperature measurements were required. At 77 K in frozen solution, the decay of the triplet excited state was found to be in the second time scale, resulting in an emission that is clearly visible up to 5 seconds after a laser excitation.

Because the europium emission is not present during this long-lived triplet emission, the sensitisation through the triplet state (T_1) of the coumarin does certainly not happen. Furthermore, both the rise time of the $^5D_1 \rightarrow {}^7F_1$ transition and the decay of the singlet state are clearly in the nanosecond time scale (<100 ns). However, a higher time resolution would be needed to quantify them precisely and thereby to determine whether an expected dependence of the rate constants on the length of the side chain is actually observed. Those data are still in agreement with a sensitisation through the singlet state of the coumarin (S_1) since the energy transfer occurs in the same time scale as the deactivation of the singlet state. Triplet–triplet transient absorption spectroscopy could provide further information that should confirm that the triplet excited state is not involved in the sensitisation of the lanthanide ion in aqueous solution and at room temperature. This hypothesis is investigated in the next section.

Transient absorption spectroscopy: time resolved T–T absorption

At room temperature, the triplet excited state of the coumarin moiety could not be observed by luminescence. In order to completely exclude the triplet excited state of the coumarin as a sensitisation pathway of the europium ion, triplet–triplet (T–T) transient absorption experiments were carried out at room temperature. 4-Methylumbelliferone has a T–T absorption between 400 nm and 550 nm.[44] Aqueous solution of the uncoupled mp3C1 chromophore (0.3 mM in Tris 0.1 M, pH 7.4) and both the gadolinium and europium complexes of dp3C1 (0.1 mM in Tris 0.1 M, pH 7.4) were excited by 355 nm nanosecond pulses (20 Hz, 6 ns, 1.5 mJ) and the transient absorption measured at 450 nm with a continuous Xenon light source perpendicular to the excitation laser.

Transient absorptions with decays in the microsecond range were measured for each solution containing the coumarin chromophore. Solutions of the parent dpa complexes yielded no transient signal. The difference between the decays of the transient absorption is weak as shown in Fig. 5 by the normalised absorption changes. An average lifetime of 2.9 μs was found.

Degassing the solution was not conclusive in showing any significant quenching that would be due to the presence of dioxygen in aerated solutions. However, the removal of oxygen sometimes has very small effects on the relaxation of the triplet

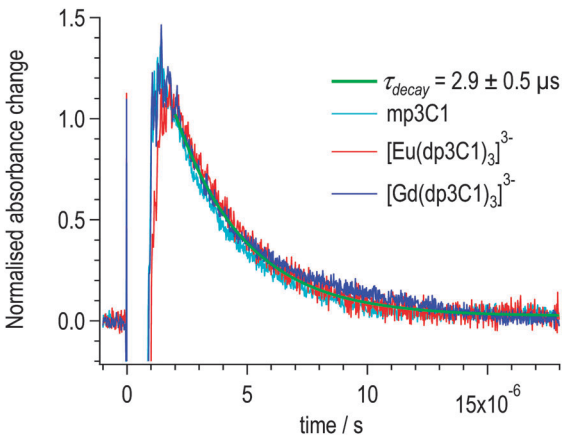

Fig. 5 Transient absorption at 450 nm after nanosecond pulsed excitation at 355 nm of aerated Tris buffered (pH 7.4) aqueous solutions of mp3C1 (0.3 mM, cyan line), $[Eu(dp3C1)_3]^{3-}$ (0.1 mM, red line) and $[Gd(dp3C1)_3]^{3-}$ (0.1 mM, blue line) at room temperature. The green line represents the fitted average exponential decay.

excited state, and particularly with water as solvent.[45,46] The attribution of this transient absorption to T–T absorptions is based on the location of the T–T absorption in 4-methylumbelliferone.[44]

Because no substantial quenching is measured between the gadolinium and europium complex, the observed excited state is certainly not involved in the sensitisation of europium. In comparison, known triplet sensitisation showed quenching by a factor of more than 2.5.[47] Moreover, a strong correlation between the relaxation rate constant of the triplet excited state and the growing rate constant of the europium luminescence is usually observed when the triplet excited state mediates energy transfer onto the lanthanide ion. In our case, no rise of the europium population was observed during the deactivation of the triplet excited state. Therefore, a sensitisation of europium *via* the triplet excited state of the coumarin moiety is unlikely to occur under such conditions.

Effect of the sensitisation on the intersystem crossing rate

In order to further confirm that the singlet excited state is involved in the sensitisation pathway, the effect of the sensitisation on the intersystem crossing rate was investigated. The population of the triplet excited state was studied at 77 K in frozen solutions. For this purpose, the emission spectra of the gadolinium dp3C1 complex $[Gd(dp3C1)_3]^{3-}$, of the europium dp3C1 complex $[Eu(dp3C1)_3]^{3-}$ and of the free dp3C1 ligand $dp3C1^{2-}$ were measured at 77 K under continuous excitation at 320 nm (see Fig. 6). The emission spectrum of the gadolinium complex shows a phosphorescence component that is exclusively observed upon time resolution. On the other hand, the europium complex has a weak phosphorescent component at this location. Under time resolution, the phosphorescence is still observed and lasts for seconds. By fitting the contribution of the time resolved phosphorescence spectra in the total emission spectra, the triplet state emission is estimated to account for 13% of the total emission of the gadolinium complex at 77 K. In the free ligand, the contribution is lower (~9%) as expected by the heavy atom effect of the lanthanide ion in the complex. The much weaker phosphorescent emission in the europium complex (~3%) compared to the gadolinium analogue indicates that the intersystem crossing rate is slower in the europium complex. This behaviour is consistent with a singlet mediated energy transfer. Since no quenching of the triplet excited state by energy transfer to the europium ion was observed by transient absorption at room temperature, and because the europium emission is not observed alongside the phosphorescent emission upon time resolution at 77 K, the triplet excited state is undeniably not mediating any energy transfer. The lower population at 77 K of the triplet excited state in the europium complex can then be accounted to a slower intersystem crossing rate due to a faster relaxation of the singlet excited state by energy transfer onto the europium ion.

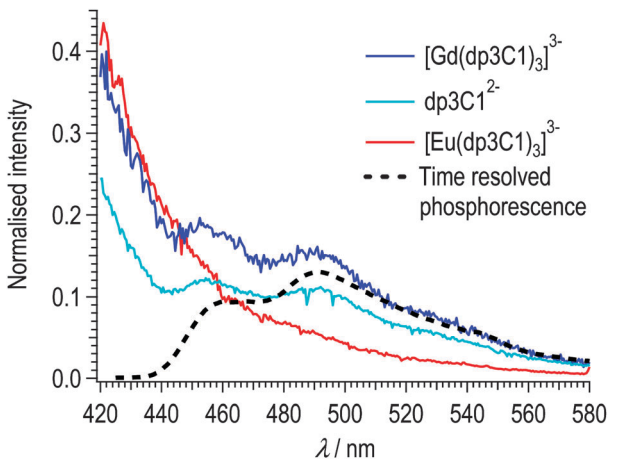

Fig. 6 Emission spectra upon continuous excitation at 320 nm of the gadolinium and europium complexes together with the free ligand in frozen solution (77 K) and compared with the time resolved phosphorescence spectrum of the coumarin.

Conclusions

In conclusion, we have been able to demonstrate with coumarin-based sensitisers that despite similar structures and energy levels, the sensitisation efficiency cannot rely only on the energetics of the excited states, but has to take into account the possible deactivations and photophysical processes that depend on the structure of each sensitiser. We have then revealed for the first time with minimal perturbations of the ligand design that a correlation between the length of the linker (POE side chain) separating the sensitiser from the lanthanide ion and the quantum yield is indeed observed in the solid state as expected by energy transfer theories, but may not show up in aqueous solution perhaps due to the flexible structure of the polyoxyethylene linker in aqueous solution. We have also shown that the sensitisation of the lanthanide ions by coumarin derivatives at low temperature is occurring mainly through the singlet excited state of the coumarin and not *via* the usual triplet pathway. No evidence for a triplet-mediated sensitisation at room temperature was found. It is therefore, the first occurrence of a relationship between the quantum yield of a sensitised lanthanide luminescence and the "distance" of the sensitiser relative to the lanthanide ion *via* a singlet pathway sensitisation. We have proved that such a ligand design is a versatile system for the investigation of sensitisers for lanthanide ion. The synthesis (see the Experimental section) of those ligands is simple: the only requirement is that the sensitiser to investigate has a nucleophilic functional group that can be grafted on a polyoxyethylene side chain. Other sensitisers may be investigated that way with minimal adaptations of the synthesis. Chromophores with known triplet pathways would be particularly interesting to test comparatively to the singlet pathway sensitisers. Besides, this simple structural design may then be a nice way to screen a library of chromophores for potential lanthanide sensitisers, and select promising candidates for an incorporation in more complex architectures with a higher density of chromophores and luminescent metal centres such as dendrimers.

Experimental section

General procedures

The solvents were purified by a non-hazardous procedure by passing them onto activated alumina columns (Innovative

Technology Inc. system). The chemicals were ordered from Fluka and Aldrich and used without further purification. The ESI-MS spectra were obtained by Dr Laure Ménin and the elemental analyses were performed by Dr E. Solari, at the École Polytechnique Fédérale de Lausanne. ^{1}H, ^{13}C and HSQC NMR spectroscopy was performed on a Bruker Avance DRX 400 spectrometer at 25 °C, using deuterated solvents as internal standards. The chemical shifts are given in ppm relative to TMS.

Photophysical measurements

The analytical grade solvents and chemicals were used without further purification. The aqueous solutions were prepared from doubly distilled water. The lanthanides solutions were prepared from the corresponding perchlorate salt and titrated by complexometry using a standardised Na_2H_2EDTA solution in a urotropine-buffered medium and with xylenol orange as an indicator.

The aqueous solutions containing lanthanide complexes were directly prepared by adding the stoichiometric amount of lanthanide ions (from a freshly titrated solution of a lanthanide salt) to a Tris-buffered aqueous solution at pH 7.4 of the diluted ligand. Aliquots of the solutions containing lanthanide complexes were titrated with a standardised Na_2H_2EDTA solution in a urotropine-buffered medium and with xylenol orange as an indicator to ensure that no free (*i.e.* uncomplexed) lanthanide ion were present in the solutions.

In order to better reproduce the properties of the prepared solid state samples, we found that drying Tris-buffered solutions instead of unbuffered solutions helped producing repeatable results. The solid state samples are then solid state complexes in a solid Tris matrix. The solid state samples were prepared by mixing 50 mg of the ligand to the stoichiometric amount (3 ligands per lanthanide) of lanthanide chloride (previously titrated to determine the hydration number) in 18 ml of hot water (90 °C), adding 2 ml of a Tris 1 M aqueous solution at pH 7.4 and slowly evaporating at room temperature the 0.1 M Tris-buffered aqueous solutions until a solid residue remained. The solid residue was then collected and further dried at 65 °C for 2 hours under slightly reduced pressure (~600 mbar). The warm samples were finally stored in a desiccator at room temperature.

The UV-Vis absorption spectra were measured on a Perkin-Elmer Cary 1E spectrophotometer using 0.2 cm path length quartz cells.

The room temperature excitation and emission spectra of the europium and gadolinium dp3Cy complexes were recorded on a Fluorolog 3-22 spectrofluorimeter from Jobin-Yvon. The room temperature excitation and emission spectra of the terbium dp3Cy complexes and of the europium and gadolinium complexes of dpxC1 were measured on a Perkin Elmer LS50B spectrofluorimeter in phosphorescence mode with a zero delay. The titration experiments were also performed on the Perkin Elmer LS50B in phosphorescence mode by integrating the intensity at 615 nm and monitoring the variation upon addition of aliquots containing 1/15 europium equivalent to a 0.1 M Tris buffered 0.3 mM ligand aqueous solution (pH 7.4). The excitation and emission spectra, as well as the titration experiments were measured in 1 cm or 0.2 cm path length quartz cells. The low temperature measurements were performed at 77 K in quartz Suprasil® capillaries with 10% glycerol added to the Tris-buffered aqueous solutions.

The quantum yields were determined in an integration sphere by measuring the ratio of the emitted corrected intensity over the absorbed corrected intensity. Empty capillaries have been used as a blank. A 75 W Xenon light source with a monochromator was used as a light source. The emissions from the integrating sphere were collected with an optical fibre and analysed on a Hamamatsu photonic multichannel analyser C8808 detector. The correction function of the setup was calculated with a calibrated standards Deuterium and Halogen light sources as reference irradiances. All concentrations were set at 0.1 mM.

The time-resolved emission spectra were measured by exciting the samples with an Ekspla NT 342/3/UV pulsed laser. The excitation wavelength was set at 320 nm and gave a 6 ns pulse of 0.53 ± 0.04 cm^2 with a typical energy of 1–5 mJ at a frequency of 20 Hz. The resulting emissions were collected with an optical fibre and analysed on a Hamamatsu photonic multichannel analyser C8808 detector.

The transient absorptions were measured in 1 cm quartz cells. Aqueous solutions were photoexcited by short light pulses (5 ns FWHM) generated by a frequency-tripled Q-switched Nd:YAG laser (Ekspla NT-340). The pump fluence was of the order of 20 mJ cm^{-2}. The probe light from a Xenon arc lamp was passed through filters, various optical elements, the sample, and a grating monochromator, before being detected by a fast photomultiplier tube and recorded by a digital oscilloscope. The kinetic traces were typically averaged over 3000–4000 consecutive laser shots.

Synthesis of the ligands

The dp3C1 ligand was synthesised from commercial 4-methylumbelliferone according to our previous procedure.[39] The other ligands were synthesised according to the following new synthesis. The tosylated oligoethylene glycol monomethyl ethers were synthesised according to the procedure in the supplementary materials of Kohmoto and *et al.*[48] Diethylchelidamate (Et_2chelida) was prepared according to a previously reported procedure.[35]

General procedure for the synthesis of 4-hydroxycoumarins

4-Hydroxycoumarins were synthesised according to Jung *et al.*[49] The corresponding 4-substituted 2-hydroxyacetophenone (50 mmol) was dissolved with diethyl carbonate (75 mmol) in toluene (25 ml). The solution was added dropwise under an inert atmosphere and at room temperature to a vigorously stirred suspension of sodium hydride (60% w/w moistened with oil, 250 mmol) in toluene (125 ml). After complete addition, the reaction was heated up to 105 °C for 3 hours. The solvent was then evaporated. Water (100 ml) was added to the residual solid to quench the excess of sodium hydride. The solution was

concentrated under vacuum to remove the remaining toluene and acidified with concentrated hydrochloric acid down to pH 1 to form a precipitate that can be filtered out, washed with water and dried *in vacuo*. Recrystallisation from ethanol can be performed to obtain higher purity 4-hydroxycoumarins if needed.

C4: ^{1}H NMR δ: 7.84 (dd, J_1 = 7.8 Hz, J_2 = 1.6 Hz, 1H), 7.66 (td, J_1 = 7.9 Hz, J_2 = 1.7 Hz, 1H), 7.37 (m, 2H), 5.62 (s, 1H).

Non commercial 2-hydroxyacetophenones like 4-chloro-2-hydroxyacetophenone can be synthesised through a Fries rearrangement of the 3-substituted acetoxybenzene, for the 4-chloro-2-hydroxyacetophenone, 3-chloroacetoxybenzene, obtained from 3-chlorophenol, was reacted with $AlCl_3$.[50]

C5: ^{1}H NMR δ: 7.83 (d, J = 8.5 Hz, 1H), 7.58 (d, J = 1.7 Hz, 1H d1 = 20 sec.), 7.42 (m, 1H), 5.65 (s, 1H).

Synthesis of 7-hydroxycoumarins. 7-Hydroxy-4-methoxycoumarin (C2) was synthesised from 4-hydroxy-7-methoxycoumarin (C3) (1 g, 5.20 mmol) by demethylation of the 7-methoxy group with hydroiodic acid (75 ml) in a 1/1 (v/v) acetic acid/acetic anhydride solution (total 60 ml) under reflux (120 °C) for 3 h 30 min. The obtained 4,7-dihydroxycoumarin (471 mg, 51%) was then remethylated selectively at position 4 by heating in methanol (0.1 M solution, 16 ml) with concentrated sulfuric acid (1.25 ml acid per mmol dihydroxycoumarin) for 1 hour and a half. 7-Hydroxy-4-methoxycoumarin (C2) is obtained as a slightly pinkish white powder (163 mg, 54% from 4,7-dihydroxycoumarin).

C2: ^{1}H NMR δ: 10.57 (s, 1H), 7.63 (d, J = 8.7 Hz, 1H), 6.80 (dd, J_1 = 8.6 Hz, J_2 = 2.2 Hz, 1H), 6.71 (d, J = 2.2 Hz, 1H), 5.69 (s, 1H), 3.98 (s, 3H). C3: ^{1}H NMR δ: 7.73 (d, J = 8.6 Hz, 1H), 6.94 (m, 2H), 5.43 (s, 1H), 3.86 (s, 3H).

Synthesis of the POEMEated coumarins. Coumarins were coupled to a polyoxyethylene chain by attacking tosylated triethylene glycol monomethyl ether (1.2 eq.) in DMF (0.3 M in coumarin) with an excess of K_2CO_3 (22 eq.) at 75 °C for 48 hours. The solvent was then evaporated, the residual slurry dissolved in dichloromethane, washed three times with half saturated NH_4Cl aqueous solution, dried with Na_2SO_4, and the solvent evaporated *in vacuo*. Purification by silica gel chromatography with ethyl acetate 100% as eluent gave the pure desired product as a solid after evaporation of the solvent. In the case of mp3C2 and mp3C3, the oily residue obtained after washing with aqueous NH_4Cl was solidified by adding a small amount of diethyl ether and sonicating at 40 °C. The white solid was filtrated, rinsed with diethyl ether and further dried to yield pure mp3Cy.

Mp3C2: yield 100%. ^{1}H NMR δ: 7.70 (d, J = 8.8 Hz, 1H), 7.02 (d, J = 2.3 Hz, 1H), 6.97 (dd, J_1 = 8.8 Hz, J_2 = 2.4 Hz, 1H), 5.77 (s, 1H), 4.22 (m, 2H), 4.00 (s, 3H), 3.78 (m, 2H), 3.61 (m, 2H), 3.55 (m, 2H), 3.52 (m, 2H), 3.43 (m, 2H), 3.24 (s, 3H). ESI-MS $C_{17}H_{23}O_7^+$, calcd 339.144 *m*/*z*, found 339.141 *m*/*z*. Mp3C3: yield 100%. ^{1}H NMR δ: 7.71 (d, J = 8.8 Hz, 1H), 7.01 (d, J = 2.3 Hz, 1H), 6.97 (dd, J_1 = 8.8 Hz, J_2 = 2.6 Hz, 1H), 5.78 (s, 1H), 4.34 (m, 2H), 3.86 (m, 5H), 3.65 (m, 2H), 3.55 (m, 4H), 3.43 (m, 2H), 3.24 (s, 3H). ESI-MS $C_{17}H_{23}O_7^+$, calcd 339.144 *m*/*z*, found 339.143 *m*/*z*. Mp3C4: yield 50%. ^{1}H NMR δ: 7.82 (dd, J_1 = 7.9 Hz, J_2 = 1.6 Hz, 1H), 7.68 (td, J_1 = 7.6 Hz, J_2 = 1.7 Hz, 1H), 7.40 (m, 2H), 5.95 (s, 1H), 4.37 (m, 2H), 3.88 (m, 2H), 3.65 (m, 2H), 3.55 (m, 4H), 3.42 (m, 2H), 3.23 (s, 3H). ESI-MS $C_{16}H_{21}O_6^+$, calcd 309.134 *m*/*z*, found 309.137 *m*/*z*. Mp3C5: yield 42%. ^{1}H NMR δ: 7.81 (d, J = 8.5 Hz, 1H), 7.62 (d, J = 2.0 Hz, 1H), 7.46 (dd, J_1 = 8.5 Hz, J_2 = 2.0 Hz, 1H), 5.98 (s, 1H), 4.37 (m, 2H), 3.87 (m, 2H), 3.65 (m, 2H), 3.56 (m, 2H), 3.53 (m, 2H), 3.42 (m, 2H), 3.23 (s, 3H). ESI-MS $C_{15}H_{20}ClO_6^+$, calcd 343.095 *m*/*z*, found 343.093 *m*/*z*.

The resulting yields are in agreement with the ability of the substituent to lower the nucleophilicity of the coupling hydroxyl group on the coumarin. Hence, an electron withdrawing group at position 7, like a chlorine (C5), diminishes the yield compared to the unsubstituted 4-hydroxycoumarin (C4). On the other hand, an electron donating group like a methoxy increases the yield up to a quantitative coupling.

Coupling of POEated coumarins with chelidamic acid. POEMEated coumarins were demethylated at the end of the POE side chain by reacting them with trimethylsilyl iodide (TMSI, 1.2 eq.) in acetonitrile (0.15 M in POEMEated coumarin). TMSI was added dropwise in the warm solution (at 75 °C) and further stirred 2 hours at 75 °C. The solvent was then evaporated, the residue dissolved in dichloromethane (DCM) and the solution washed with $Na_2S_2O_3$ (0.09 M, 20 mmol $Na_2S_2O_3$ per mmol TMSI). The aqueous phase was then further extracted with DCM (2 times) and the collected organic layers dried over Na_2SO_4, filtered and evaporated under reduced pressure to yield the crude product used without purification in the next step.

Mitsunobu reaction with resin supported TPP. Diethylchelidamate (Et_2chelida) was dissolved in DCM (0.06 M in Et_2chelida) with the POEated coumarin (1.5 eq.) and resin supported triphenylphosphine (PS-TPP, 1.5 eq.). The dispersion was cooled down to 0 °C and diisopropylazodicarboxylate (DIAD, 1.5 eq.) was then added dropwise to the cold stirred solution. The reaction was then allowed to warm at room temperature and stirred for 5 hours. The solution was then filtered to remove the TPP resin. The resin was washed with DCM (50 ml) and the filtrate was washed with aqueous HCl 1M (50 ml) once and three times with H_2O (3 × 50 ml). The organic layer was dried with Na_2SO_4, filtered and evaporated under reduced pressure to yield on oil composed of the coupled desired product together with residual uncoupled POEated coumarin. The excess of POE containing coumarin is removed in the next step. The crude product was then used without further purification in the final step.

Deprotection of the carboxylic acid by hydrolysis of the diethyl ester moiety. The diesters groups of the POE coupled coumarin are removed by hydrolysis with aqueous NaOH in EtOH. The diethyl ester is first dissolved in ethanol (0.08 M) and aqueous NaOH (2.2 eq., 0.5 M in NaOH) added dropwise to the stirred solution at room temperature. A precipitate gently appears after the NaOH addition. The reaction mixture is further stirred for 30 minutes. The product is then isolated in the form of the sodium dicarboxylate salt.

The pure sodium dicarboxylate salt is obtained by recrystallisation of the precipitate in ethanol with a minimum amount of water followed by filtration. The filtered solid is washed with cold ethanol and collected as a wet powder. The powder is then

dried *in vacuo* to obtain the desired ligand. It is characterised by ^{1}H-NMR and ^{13}C-NMR in D_2O and by elemental analysis.

Na_2dp3C2: ^{1}H NMR (400 MHz, D_2O) δ 7.48 (d, 1H, J = 8.4 Hz), 7.20 (s, 2H), 6.80 (m, 2H), 5.43 (s, 1H), 4.18 (m, 2H), 4.00 (m, 2H), 3.85 (m, 5H), 3.80 (m, 2H), 3.74 (m, 2H), 3.67 (m, 2H). ^{13}C NMR (101 MHz, D_2O) δ 171.9 ($C_{carboxylate}$), 168.0 ($^{4Coum}C_{ar}$–O), 166.6 ($^{4pyr}C_{ar}$–O), 166.0 ($^{7Coum}C_{ar}$–O), 161.7 ($^{2Coum}C_{ar}$═O), 154.2 ($^{(2+6)pyr}C_{ar}$), 153.6 ($^{(8-1)\text{-}bridgeCoum}C_{ar}$), 124.0 ($^{5Coum}C_{ar}$–H), 112.8 ($^{6Coum}C_{ar}$–H), 111.1 ($^{(3+5)pyr}C_{ar}$–H), 108.3 ($^{(4-5)\text{-}bridgeCoum}C_{ar}$), 100.7 ($^{8Coum}C_{ar}$–H), 86.3 ($^{3Coum}C_{ar}$–H), 69.9 ($OCH_2$–C–$H_2$), 69.8 ($OCH_2$–C–$H_2$), 68.7 ($OCH_2$–C–$H_2$), 68.6 ($OCH_2$–C–$H_2$), 67.4 ($OCH_2$–C–$H_2$), 67.3 ($OCH_2$–C–$H_2$), 56.6 (O–C–$H_3$). $Na_2C_{23}H_{21}NO_{11}\cdot 2NaOH$ (613.40): calcd C 45.04, H 3.78, N 2.28; found C 45.05, H 3.87, N 2.15. ESI-MS: $C_{23}H_{24}NO_{11}^+$ calcd 490.1349 *m*/*z*, found 490.1348 *m*/*z*. Na_2dp3C3: ^{1}H NMR (400 MHz, D_2O) δ 7.27 (d, J = 8.9 Hz, 1H), 7.05 (s, 2H), 6.49 (dd, J = 2.5, 8.9 Hz, 1H), 6.33 (d, J = 2.4 Hz, 1H), 5.32 (s, 1H), 4.12 (m, 2H), 3.99 (m, 2H), 3.87 (m, 2H), 3.79 (m, 2H), 3.74 (m, 2H), 3.69 (m, 2H), 3.62 (s, 3H). ^{13}C NMR (101 MHz, D_2O) δ 171.8 ($C_{carboxylate}$), 167.1 ($^{4Coum}C_{ar}$–O), 166.5 ($^{4pyr}C_{ar}$–O), 165.9 ($^{7Coum}C_{ar}$–O), 162.7 ($^{2Coum}C_{ar}$═O), 154.1 ($^{(2+6)pyr}C_{ar}$), 153.8 ($^{(8-1)\text{-}bridgeCoum}C_{ar}$), 124.0 ($^{6Coum}C_{ar}$–H), 112.5 ($^{5Coum}C_{ar}$–H), 110.9 ($^{(3+5)pyr}C_{ar}$–H), 108.0 ($^{(4-5)\text{-}bridgeCoum}C_{ar}$), 99.9 ($^{8Coum}C_{ar}$–H), 86.9 ($^{3Coum}C_{ar}$–H), 70.2 ($OCH_2$–C–$H_2$), 69.9 ($OCH_2$–C–$H_2$), 68.7 ($OCH_2$–C–$H_2$), 68.5 ($OCH_2$–C–$H_2$), 68.2 ($OCH_2$–C–$H_2$), 67.3 ($OCH_2$–C–$H_2$), 55.7 (O–C–$H_3$). $Na_2C_{23}H_{21}NO_{11}\cdot 2.3NaOH$ (625.40): calcd C 44.17, H 3.76, N 2.24; found C 44.19, H 3.62, N 2.52. ESI-MS: $C_{23}H_{24}NO_{11}^+$ calcd 490.1349 *m*/*z*, found 490.1352 *m*/*z*. Na_2dp3C4: ^{1}H NMR (400 MHz, D_2O) δ 7.91 (m, 1H), 7.62 (m, 1H), 7.40 (m, 2H), 7.33 (m, 2H), 5.91 (m, 1H), 4.49 (m, 2H), 4.26 (m, 2H), 4.12 (m, 2H), 4.01 (m, 2H), 3.94 (m, 2H), 3.89 (m, 2H). ^{13}C NMR (101 MHz, D_2O) δ 172.0 ($C_{carboxylate}$), 166.8 ($^{4Coum}C_{ar}$–O), 166.1 ($^{4pyr}C_{ar}$–O), 166.0 ($^{2Coum}C_{ar}$═O), 154.3 ($^{(2+6)pyr}C_{ar}$), 152.0 ($^{(8-1)\text{-}bridgeCoum}C_{ar}$), 133.0 ($^{7Coum}C_{ar}$–H), 124.6 ($^{6Coum}C_{ar}$–H), 122.8 ($^{5Coum}C_{ar}$–H), 116.4 ($^{8Coum}C_{ar}$–H), 114.6 ($^{(4-5)\text{-}bridgeCoum}C_{ar}$), 111.0 ($^{(3+5)pyr}C_{ar}$–H), 89.4 ($^{3Coum}C_{ar}$–H), 70.1 ($OCH_2$–C–$H_2$), 69.8 ($OCH_2$–C–$H_2$), 68.6 (2× OCH_2–C–H_2), 68.2 (OCH_2–C–H_2), 67.3 (OCH_2–C–H_2). $Na_2C_{22}H_{19}NO_{10}\cdot 0.85NaOH\cdot 0.25CH_3CH_2OH$ (548.89): calcd C 49.24, H 3.92, N 2.55; found C 49.24, H 3.97, N 2.48. ESI-MS: $C_{22}H_{22}NO_{10}^+$ calcd 460.1244 *m*/*z*, found 460.1243 *m*/*z*. Na_2dp3C5: ^{1}H NMR (400 MHz, D_2O) δ 7.45 (m, 1H), 7.08 (m, 2H), 7.01 (m, 2H), 5.56 (s, 1H), 4.22 (m, 2H), 4.04 (m, 2H), 3.92 (m, 2H), 3.82 (m, 2H), 3.76 (m, 2H), 3.72 (m, 2H). ^{13}C NMR (101 MHz, D_2O) δ 171.7 ($C_{carboxylate}$), 166.0 ($^{4Coum}C_{ar}$–O), 165.9 ($^{4pyr}C_{ar}$–O), 165.3 ($^{2Coum}C_{ar}$═O), 154.1 ($^{(2+6)pyr}C_{ar}$), 152.0 ($^{(8-1)\text{-}bridgeCoum}C_{ar}$), 138.1 ($^{7Coum}C_{ar}$–Cl), 124.9 ($^{5Coum}C_{ar}$–H), 124.1 ($^{6Coum}C_{ar}$–H), 116.4 ($^{8Coum}C_{ar}$–H), 113.2 ($^{(4-5)\text{-}bridgeCoum}C_{ar}$), 110.9 ($^{(3+5)pyr}C_{ar}$–H), 89.4 ($^{3Coum}C_{ar}$–H), 70.2 ($OCH_2$–C–$H_2$), 70.0 ($OCH_2$–C–$H_2$), 68.9 ($OCH_2$–C–$H_2$), 68.7 ($OCH_2$–C–$H_2$), 68.2 ($OCH_2$–C–$H_2$), 67.4 ($OCH_2$–C–$H_2$). $Na_2C_{22}H_{18}ClNO_{10}\cdot 0.4CH_3CH_2OH$ (556.25): calcd C 49.23, H 3.70, N 2.52; found C 49.30, H 3.68, N 2.30. ESI-MS: $C_{22}H_{21}ClNO_{10}^+$ calcd 494.0854 *m*/*z*, found 494.0855 *m*/*z*.

Synthesis of the dpxC1 ligands. The variation of the length of the POE side chain was performed by replacing the tosylated triethylene glycol monomethyl ether from the synthesis of the dp3Cy ligands by the desired oligoethylene glycol derivative, *i.e.* tosylated diethylene glycol monomethyl ether for dp2C1 and tosylated ethylene glycol monomethyl ether for dp1C1, according to the same synthetic pathway.

Na_2dp2C1: ^{1}H NMR (400 MHz, D_2O) δ 7.45 (d, 1H, J = 8.8 Hz), 7.30 (s, 2H), 6.88 (d, 1H, J = 2.3 Hz), 6.82 (dd, 1H, J = 8.8, 2.4 Hz), 6.10 (s, 1H), 4.33 (m, 2H), 4.22 (m, 2H), 3.99 (m, 4H), 2.32 (s, 3H). ^{13}C NMR (HSQC) δ 126.1 ($^{5Coum}C_{ar}$–H), 113.9 ($^{6Coum}C_{ar}$–H), 111.2 ($^{(3+5)pyr}C_{ar}$–H), 110.2 ($^{8Coum}C_{ar}$–H), 101.7 ($^{3Coum}C_{ar}$–H), 68.8 (OCH_2–C–H_2), 68.6 (OCH_2–C–H_2), 67.6 (OCH_2–C–H_2), 67.4 (OCH_2–C–H_2), 17.9 ($^{4Coum}C_{ar}$–C–H_3). $Na_2C_{21}H_{17}NO_9\cdot 2.0NaOH$ (553.34): calcd C 45.58, H 3.46, N 2.53; found C 45.56, H 3.20, N 2.77. Na_2dp1C1: ^{1}H NMR (400 MHz, D_2O) δ 7.57 (d, 1H, J = 8.9 Hz), 7.47 (s, 2H), 6.94 (d, 1H, J = 8.8 Hz), 6.90 (s, 1H), 6.11 (s, 1H), 4.53 (m, 2H), 4.48 (m, 2H), 2.34 (s, 3H). ^{13}C NMR (HSQC) δ 125.9 ($^{5Coum}C_{ar}$–H), 113.1 ($^{6Coum}C_{ar}$–H), 111.4 ($^{(3+5)pyr}C_{ar}$–H), 110.3 ($^{8Coum}C_{ar}$–H), 101.8 ($^{3Coum}C_{ar}$–H), 67.0 (OCH_2–C–H_2), 66.8 (OCH_2–C–H_2), 18.0 ($^{4Coum}C_{ar}$–C–H_3). $Na_2C_{19}H_{13}NO_8\cdot 2.0H_2O$ (465.33): calcd C 49.04, H 3.68, N 3.01; found C 49.02, H 3.69, N 2.94.

Acknowledgements

The authors would like to thank the group of photochemical dynamics headed by Prof. Jacques Moser at the EPFL for hosting and granting us access to lasers and time resolved equipment, as well as Jelissa De Jonghe for her help with the transient absorption setup.

Notes and references

1 S. V. Eliseeva and J. C. G. Bunzli, *New J. Chem.*, 2011, **35**, 1165–1176.
2 S. V. Eliseeva and J. C. G. Bunzli, *Chem. Soc. Rev.*, 2010, **39**, 189–227.
3 K. Binnemans, *Chem. Rev.*, 2009, **109**, 4283–4374.
4 J. Andres and A.-S. Chauvin, *Lanthanides: Luminescence, to be published in: The Rare Earths: Fundamentals and Applications*, Wiley, Chichester, 2012.
5 D. Parker, R. S. Dickins, H. Puschmann, C. Crossland and J. A. K. Howard, *Chem. Rev.*, 2002, **102**, 1977–2010.
6 J. P. Cross, M. Lauz, P. D. Badger and S. Petoud, *J. Am. Chem. Soc.*, 2004, **126**, 16278–16279.
7 D. L. Dexter, *J. Chem. Phys.*, 1953, **21**, 836–850.
8 T. Forster, *Discuss. Faraday Soc.*, 1959, 7–17.
9 A. Olaya-Castro and G. D. Scholes, *Int. Rev. Phys. Chem.*, 2011, **30**, 49–77.
10 V. May, *Dalton Trans.*, 2009, 10086–10105.
11 M. D. Ward, *Coord. Chem. Rev.*, 2010, **254**, 2634–2642.
12 O. L. Malta, *J. Lumin.*, 1997, **71**, 229–236.
13 M. Kleinerman, *J. Chem. Phys.*, 1969, **51**, 2370–2381.
14 I. M. Clarkson, A. Beeby, J. I. Bruce, L. J. Govenlock, M. P. Lowe, C. E. Mathieu, D. Parker and K. Senanayake, *New J. Chem.*, 2000, **24**, 377–386.
15 M. Latva, H. Takalo, V. M. Mukkala, C. Matachescu, J. C. RodriguezUbis and J. Kankare, *J. Lumin.*, 1997, **75**, 149–169.

16 N. M. Shavaleev, S. V. Eliseeva, R. Scopelliti and J. C. G. Bunzli, *Chem.–Eur. J.*, 2009, **15**, 10790–10802.
17 G. A. Hebbink, S. I. Klink, L. Grave, P. G. B. O. Alink and F. C. J. M. van Veggel, *ChemPhysChem*, 2002, **3**, 1014–1018.
18 J. R. G. Thorne, J. M. Rey, R. G. Denning, S. E. Watkins, M. Etchells, M. Green and V. Christou, *J. Phys. Chem. A*, 2002, **106**, 4014–4021.
19 C. Yang, L. M. Fu, Y. Wang, J. P. Zhang, W. T. Wong, X. C. Ai, Y. F. Qiao, B. S. Zou and L. L. Gui, *Angew. Chem., Int. Ed.*, 2004, **43**, 5010–5013.
20 J. C. G. Bunzli, A. S. Chauvin, H. K. Kim, E. Deiters and S. V. Eliseeva, *Coord. Chem. Rev.*, 2010, **254**, 2623–2633.
21 A. S. Chauvin, F. Gumy, D. Imbert and J. C. G. Bunzli, *Spectrosc. Lett.*, 2004, **37**, 517–532.
22 M. T. Alonso, E. Brunet, C. Hernandez and J. C. Rodriguezubis, *Tetrahedron Lett.*, 1993, **34**, 7465–7468.
23 M. T. Alonso, E. Brunet, O. Juanes and J. C. Rodriguez-Ubis, *J. Photochem. Photobiol., A*, 2002, **147**, 113–125.
24 C. Féau, E. Klein, P. Kerth and L. Lebeau, *Synth. Met.*, 2009, **159**, 528–536.
25 J. C. Rodriguez-Ubis, M. T. Alonso, O. Juanes and E. Brunet, *Luminescence*, 2000, **15**, 331–340.
26 S. G. Roh, N. S. Baek, K. S. Hong and H. K. Kim, *Bull. Korean Chem. Soc.*, 2004, **25**, 343–344.
27 P. G. Tarassoff and N. Filipescu, *J. Chem. Soc., Chem. Commun.*, 1975, 208–209.
28 C. Féau, E. Klein, C. Dosche, P. Kerth and L. Lebeau, *Org. Biomol. Chem.*, 2009, **7**, 5259–5270.
29 C. Féau, E. Klein, P. Kerth and L. Lebeau, *Bioorg. Med. Chem. Lett.*, 2007, **17**, 1499–1503.
30 E. Pershagen, J. Nordholm and K. E. Borbas, *J. Am. Chem. Soc.*, 2012, **134**, 9832–9835.
31 J. Y. Chen and P. R. Selvin, *J. Photochem. Photobiol., A*, 2000, **135**, 27–32.
32 M. Li and P. R. Selvin, *J. Am. Chem. Soc.*, 1995, **117**, 8132–8138.
33 P. R. Selvin, J. Jancarik, M. Li and L. W. Hung, *Inorg. Chem.*, 1996, **35**, 700–705.
34 G. Vereb, E. Jares-Erijman, P. R. Selvin and T. M. Jovin, *Biophys. J.*, 1998, **74**, 2210–2222.
35 A. L. Gassner, C. Duhot, J. C. G. Bunzli and A. S. Chauvin, *Inorg. Chem.*, 2008, **47**, 7802–7812.
36 A. D'Aleo, A. Picot, A. Beeby, J. A. G. Williams, B. Le Guennic, C. Andraud and O. Maury, *Inorg. Chem.*, 2008, **47**, 10258–10268.
37 H. Tadokoro, Y. Chatani, T. Yoshihara, S. Tahara and S. Murahashi, *Makromol. Chem.*, 1964, **73**, 109–127.
38 P. G. de Gennes, *Adv. Colloid Interface Sci.*, 1987, **27**, 189–209.
39 J. Andres and A. S. Chauvin, *Eur. J. Inorg. Chem.*, 2010, 2700–2713.
40 R. M. Supkowski and W. D. Horrocks, *Inorg. Chim. Acta*, 2002, **340**, 44–48.
41 M. H. V. Werts, R. T. F. Jukes and J. W. Verhoeven, *Phys. Chem. Chem. Phys.*, 2002, **4**, 1542–1548.
42 D. S. Mcclure, *J. Chem. Phys.*, 1949, **17**, 905–913.
43 A. Aebischer, F. Gumy and J. C. G. Bunzli, *Phys. Chem. Chem. Phys.*, 2009, **11**, 1346–1353.
44 B. R. Henry and E. A. Lawler, *J. Mol. Spectrosc.*, 1973, **48**, 117–123.
45 C. Schweitzer and R. Schmidt, *Chem. Rev.*, 2003, **103**, 1685–1757.
46 C. B. Nielsen, M. Johnsen, J. Arnbjerg, M. Pittelkow, S. P. McIlroy, P. R. Ogilby and M. Jorgensen, *J. Org. Chem.*, 2005, **70**, 7065–7079.
47 A. Beeby, S. Faulkner, D. Parker and J. A. G. Williams, *J. Chem. Soc., Perkin Trans. 2*, 2001, 1268–1273.
48 S. Kohmoto, E. Mori and K. Kishikawa, *J. Am. Chem. Soc.*, 2007, **129**, 13364.
49 J. C. Jung, Y. J. Jung and O. S. Park, *Synth. Commun.*, 2001, **31**, 1195–1200.
50 J. I. Luengo and J. D. Elliott, 2002. *U.S. Pat.*, 6353116, filed Dec. 14, 1999.

